JOURNAL OF CATALYSIS **105**, 483–498 (1987)

Selective Oxidative Dehydrogenation of Butane over V–Mg–O Catalysts

M. A. CHAAR,[1] D. PATEL, M. C. KUNG, AND H. H. KUNG[2]

Ipatieff Laboratory and Department of Chemical Engineering, Northwestern University, Evanston, Illinois 60201

Received September 3, 1986; revised January 6, 1987

Vanadium–magnesium oxides were found to be selective oxidative dehydrogenation catalysts for butane. The selectivity for dehydrogenation increased with increasing vanadium content until an optimum was reached for samples containing 24 to 54 wt% V_2O_5. Infrared spectroscopy, X-ray diffraction, Auger electron spectroscopy, and scanning electron microscopy studies of the catalysts suggested that the active component was the compound magnesium orthovanadate. For a given catalyst at about 540°C, the selectivity for oxidative dehydrogenation increased with decreasing oxygen-to-butane ratio, decreasing conversion, and decreasing temperature. A selectivity of up to 60% was obtained. The high selectivity for oxidative dehydrogenation instead of oxygenate production is attributed to two factors: the basic surface facilitates desorption of basic butenes and butadiene, and the absence of V=O lowers the oxidation activity of the surface.

INTRODUCTION

Selective oxidative dehydrogenation of alkanes is a challenging problem, because alkanes are generally much less reactive than the dehydrogenated products such as alkenes and dienes. At the high temperatures required to activate alkanes, the dehydrogenated products react rapidly with oxygen to form combustion products.

A suitable catalyst can overcome this limitation. It may provide a controlled source of highly reactive oxygen which can activate alkanes at a lower temperature at which dehydrogenation products do not react too rapidly. It may also reduce the reactivity of these products by reducing their residence time on the catalyst surface.

One approach that has been successfully demonstrated by Lunsford and co-workers is the use of N_2O as the oxidant and the controlled source of highly reactive oxygen. Selective dehydrogenation of ethane to ethene was accomplished over a silica-supported molybdena catalyst at 400°C (*1*). N_2O is decomposed over the catalyst to form adsorbed O^-, which is very reactive and abstracts a hydrogen atom from ethane. In fact, with N_2O as the oxidant, methane has been selectively oxidized to methanol and formaldehyde over supported molybdena (*2–4*) and vanadia catalysts (*5*).

There have been few reports on the use of oxygen to achieve high selectivity in the oxidative dehydrogenation of alkanes. Among the few reported, Mg–Mo–O, Ni–Mo–O (*6*), and Co–Mo–O (*7*) are shown to have respectable selectivity. We report here our study of this reaction for butane over V–Mg–O catalysts. Under appropriate conditions, a selectivity for dehydrogenation to butenes and butadiene of 60% has been achieved.

MgO is known to be selective for dehydrogenation, but its activity is low (*6*). On the other hand, vanadium oxide is active for the oxidation of butane, but the selectivity is only about 10% (*8, 9*). V–Mg–O has

---

[1] Present address: Faculty of Chemical and Petroleum Engineering, Baath University, P.O. Box 77, Homs, Syria.

[2] To whom correspondence should be addressed.

0021-9517/87 $3.00

been tested for other oxidative dehydrogenation reactions. It is very selective for the conversion of ethylbenzene to styrene (*10, 11*) and quite selective for butene to butadiene (*12*). However, to our knowledge, there has been no report on the use of V–Mg–O catalysts for the oxidative dehydrogenation of alkanes.

In this paper, we report the results of the physical characterization of the V–Mg–O catalysts to identify the active component, and the dependence of the reaction characteristics on the process variables.

EXPERIMENTAL

MgO was prepared by precipitation from a magnesium nitrate (Fisher Scientific) solution with ammonium carbonate (Alfa Products). The pH of the solution was kept at 6.5–7.0. The precipitate was suction-filtered, washed with doubly distilled water four to five times, air dried at 80°C for 24 h, and then calcined in air at 700°C for 3 h. The resultant white solid was ground into a fine powder.

Vanadium oxide was prepared by air calcination of ammonium vanadate (NH_4VO_3, Johnson Matthey, 99%) at 550°C for 3 h.

For the mixed oxide catalysts, an appropriate amount of MgO powder was added to an aqueous solution containing 0.5 wt% ammonium vanadate and 1 wt% ammonium hydroxide at 70°C. With stirring, the suspension was evaporated to dryness. The resulting solid was calcined at 550°C for 6 h. This solid was lightly crushed to break up the crumbs and used as a catalyst. The BET areas were determined by nitrogen adsorption in a static system. The actual compositions were determined by atomic absorption spectroscopy after the catalysts were dissolved in 0.1 *M* nitric acid. The reaction was carried out in a conventional flow system with a quartz U-tube reactor at close to atmospheric pressure.

Under the standard condition, the feed was 4 vol% butane (Linde, CP grade), 4 to 8% oxygen (Linde, hydrocarbon free), and the balance He (Matheson, zero grade). The flow rate was about 100 ml/min, and the reaction temperature was 480 to 600°C. The catalyst was supported by quartz wool. Unless specified, the catalyst was mixed with twice the weight of silica (<70 mesh, Davison 62). Normally, 0.1 to 0.3 g of catalyst was used. The empty reactor showed no activity, and the results were very similar with and without the use of silica diluent. In a typical reaction run, the reactor was heated to the desired temperature in the flow of reactants. The system was allowed to stabilize for about 1 h at the reaction temperature before the first product analysis was made. A typical run lasted for about 3 h. No deactivation of the catalyst was observed, and the catalyst could be reused without additional treatment. The 19V–Mg–O and 24V–Mg–O catalysts had been used for up to 10 consecutive experiments without any apparent change in their catalytic behavior.

The reaction products were analyzed by on-line gas chromatography. A Hewlett–Packard 5720A gas chromatograph equipped with a thermal conductivity detector was used. Helium was the carrier gas. A switching valve directed a pulse of reaction products into the gas chromatograph. Two columns were used in parallel. A 20-ft $\frac{1}{8}$-in.-o.d. VZ-7 (60/80 mesh, Alltech Associates, Inc.) column was used at 313 K to separate the hydrocarbons and CO_2. A 6-ft $\frac{1}{8}$-in. molecular sieve 5A column was used to separate O_2 and CO.

Infrared spectra were obtained with a Nicolet 60 SX FTIR. The catalyst as prepared was mixed with KBr and pressed into a thin wafer. Auger spectra were taken with a Physical Electronics single-pass CMA. A small amount of the powder catalyst was pressed onto an indium foil which was then mounted into the vacuum chamber. An electron energy of 3 keV was used. X-ray diffraction was performed on a Rigaku diffractometer with Cu radiation. Scanning electron microscopy was performed on a Hitachi S-510 scanning electron microscope. The samples were prepared by sprinkling the powder lightly onto a double-sided adhesive tape which was mounted on a SEM specimen stub. The edge of the double-sided tape was painted with silver paint to minimize charging. Finally, the sample was sputtered coated with gold. Micrographs were obtained in a secondary electron imaging mode using a potential difference of 25 kV. These studies were performed on the fresh catalysts.

Visual observation did not detect any changes in the appearance of the catalyst after use, provided that oxygen was not totally consumed by the reaction. However, if oxygen was totally consumed, the portion of the catalyst closer to the outlet of the reactor became gray in color, which possibly indicated reduction of vanadium to an oxidation state lower than 5 and/or deposition of coke on the catalyst.

RESULTS

Catalyst Characterization

Table 1 lists the compositions and the surface areas of the catalysts used. The number in the catalyst label denotes the approximate weight percentage of V_2O_5. As prepared, the color of the catalyst ranged from white for MgO and for those of low vanadium content, to slightly yellow for those of high vanadium content. The color of the catalysts did not change after reaction studies.

TABLE 1

Compositions and Surface Areas of the Catalysts

Catalyst	Surface area (m^2/g)	Composition			
		MgO (wt%)	V_2O_5 (wt%)	MgO (mol%)	V_2O_5 (mol%)
MgO	28	100	0	100	0
V_2O_5	3.5	0	100	0	100
3V–Mg–O	82	96.5	3.5	99.2	0.8
8V–Mg–O	91	92.1	7.9	98.1	1.9
19V–Mg–O	46[a]	81.1	18.9	95.1	4.9
24V–Mg–O	74	76.3	23.7	93.6	6.4
35V–Mg–O	51	64.9	35.1	89.3	10.7
54V–Mg–O	49	46.3	53.6	79.6	20.4

[a] Value for a used catalyst.

Results of X-ray diffraction are shown in Table 2. Up to a vanadium content of 24 wt%, only MgO diffraction lines were detected. At this composition, if all the vanadium in the catalyst reacted with MgO to form magnesium orthovanadate, $Mg_3(VO_4)_2$, the catalyst would contain about 8 mol% orthovanadate. This corresponded roughly to the detection limit of the X-ray diffraction technique used. In samples containing a higher vanadium content, diffraction lines of MgO and magnesium orthovanadate were detected. Other possible compounds of V–Mg–O, such as MgV_2O_6 and $Mg_2V_2O_7$, were not detected. For the 54V–Mg–O sample, a diffraction line that corresponded to a *d* spacing of 1.51 Å was detected. V_2O_5 had a diffraction line at this position. However, the more intense lines for V_2O_5 at 4.38 and 3.40 Å were not detected. Thus the assignment of this line to V_2O_5 was in doubt.

The infrared spectra of V_2O_5 and the catalysts in the region 400 to 1200 cm^{-1} are shown in Fig. 1. In these spectra, the contribution from MgO had been subtracted. Inspection of these spectra showed that the 1022 cm^{-1} peak characteristic of bulk V_2O_5 was missing in all of the V–Mg–O samples. The spectra of the samples of low vanadium content differed from those of high vanadium content. The spectrum of 8V–Mg–O consisted of three broad peaks at 895, 731, and 550 cm^{-1}. That for the 19V–Mg–O was quite complex and contained at least peaks at 903, 867, 820, 743, 709, and 535 cm^{-1}. Spectra for the 24V–Mg–O sample and those of higher vanadium content appeared similar. They consisted mainly of two broad and intense peaks. One was centered around 852 cm^{-1} for the 54V–Mg–O sample and shifted to about 860 cm^{-1} for the 24V–Mg–O sample. The second broad peak was composed of two peaks at 690 and 718 cm^{-1}. The 690 cm^{-1} peak was more dominant on 54V–Mg–O, whereas the 720 cm^{-1} peak was more dominant on 24V–Mg–O.

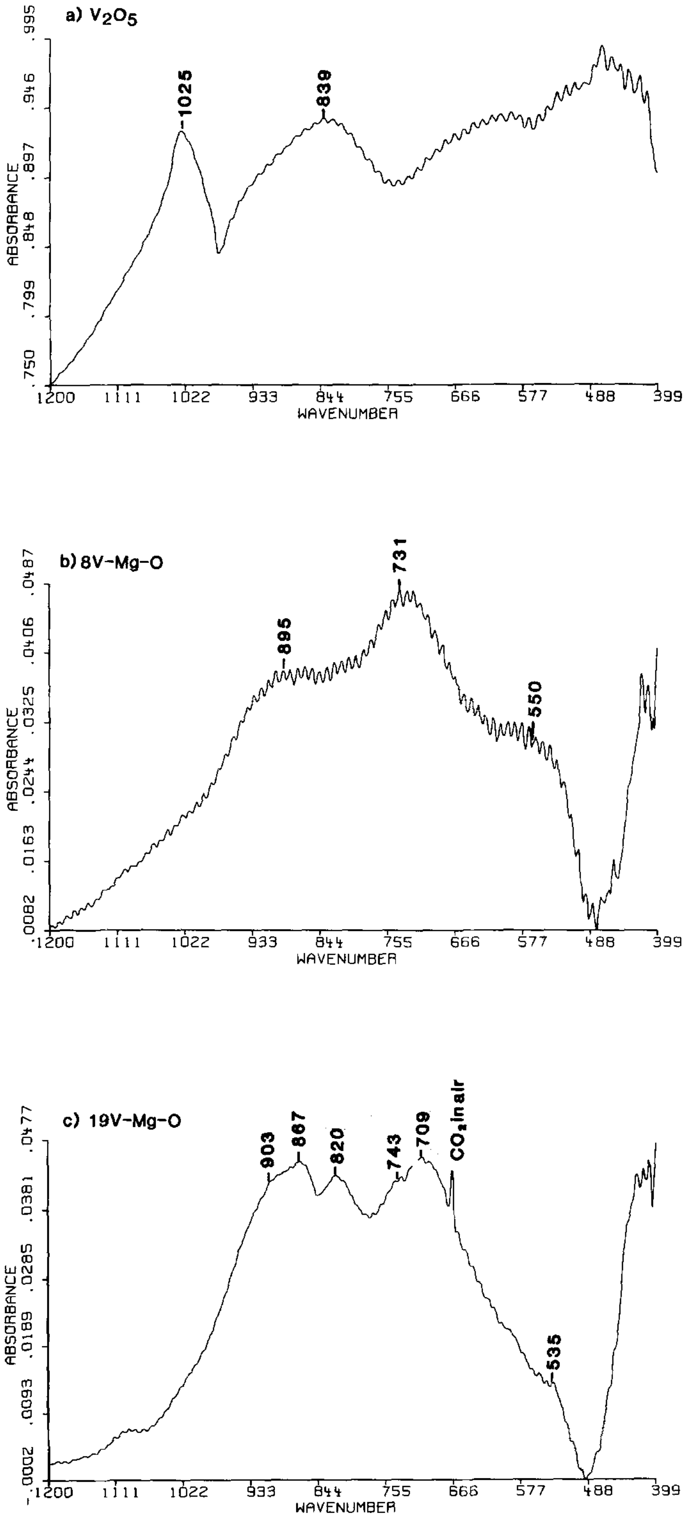

FIG. 1. Infrared spectra of (a) V_2O_5, (b) 8V–Mg–O, (c) 19V–Mg–O, (d) 24V–Mg–O, (e) 35V–Mg–O, and (f) 54V–Mg–O. In the V–Mg–O samples, the contribution from MgO has been subtracted.

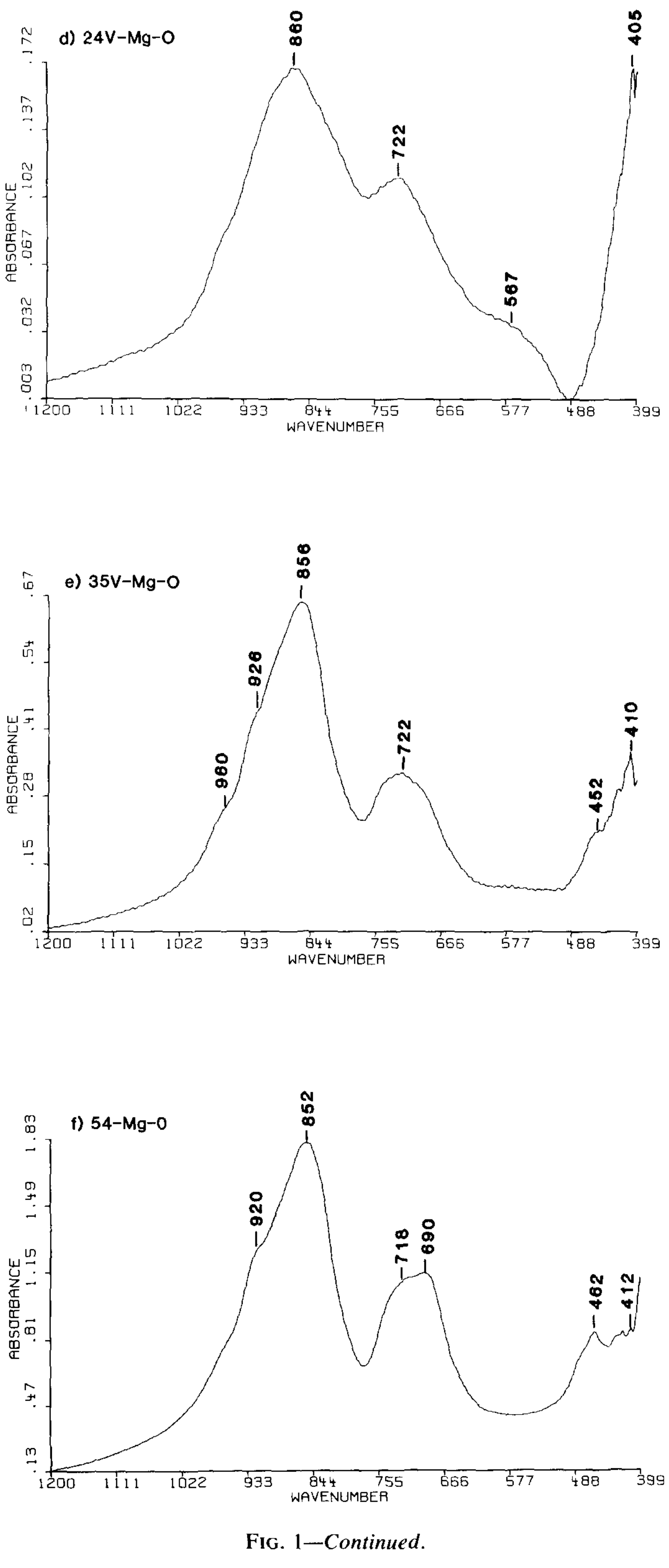

FIG. 1—*Continued.*

TABLE 2

X-ray Diffraction Lines from V–Mg–O and Their Assignments

d spacing (Å) (relative intensity)					
8V–Mg–O	19V–Mg–O	24V–Mg–O	35V–Mg–O	54V–Mg–O	Assignment[a]
				3.29(22)	$Mg_3V_2O_8$
			3.03(7)	3.02(34)	$Mg_3V_2O_8$
			2.87(5)	2.86(23)	$Mg_3V_2O_8$
			2.54(22)	2.55(100)	$Mg_3V_2O_8$
			2.49(7)	2.49(44)	$Mg_3V_2O_8$
2.43(6)	2.42(4)	2.43(6)			MgO
2.10(100)	2.10(100)	2.10(100)	2.10(100)	2.10(61)[b]	MgO
				2.08(71)	$Mg_3V_2O_8$
			1.71(2)	1.71(10)	$Mg_3V_2O_8$
			1.58(3)	1.58(13)	$Mg_3V_2O_8$
				1.51(23)	V_2O_5 (?)
1.49(57)	1.49(53)	1.49(53)	1.49(60)	1.49(46)	MgO
				1.47(68)	$Mg_3V_2O_8$
				1.43(10)	$Mg_3V_2O_8$
1.269(5)	1.269(5)	1.270(5)	1.27(3)		MgO
1.216(13)	1.218(12)	1.215(11)	1.22(10)		MgO
1.053(5)	1.053(5)	1.052(5)			MgO
				1.04(7)	$Mg_3V_2O_8$
0.966(2)	0.966(3)				MgO
0.942(13)	0.943(12)		0.94(16)		MgO

[a] Made according to the published diffraction patterns, Joint Committee for Powder Diffraction Standards, Swarthmore, Pennsylvania. Powder diffraction file card Nos. 9-387 (V_2O_5), 23-1233 (MgV_2O_6), 29-877 ($Mg_2V_2O_7$), 19-779 ($Mg_3V_2O_8$), and 4-829 (MgO). For $Mg_3V_2O_8$, the data of A. Durif [*Anal. Chem.* **31**, 1741 (1959)] were also used.

[b] A broad peak.

Shoulders at 960 and 920 cm^{-1} were also observed. A shoulder at 567 cm^{-1} was also observed on 24V–Mg–O, but not on the samples of higher vanadium content.

The surface compositions of the V–Mg–O samples were determined by Auger electron spectroscopy. The peak-to-peak intensities of the 1186-eV peak of Mg, the 510-eV peak of O, and the 473-eV peak of vanadium were measured. These intensities were then corrected for the sensitivity factors for the elements, which were 0.45 for V, 0.1 for Mg, and 0.5 for O (*13*). The ratios of the peak intensities after correction for sensitivity are listed in Table 3. The V/Mg ratio increased with increasing vanadium content up to 35% V. Beyond 35% V, the V/Mg ratio remained constant. The V/O ratio also increased with increasing V content, whereas the Mg/O ratio decreased. Beyond about 35% vanadium, these ratios became constant.

The results of the scanning electron

TABLE 3

Surface Atomic Ratios in V–Mg–O Catalysts[a]

Catalyst	V/Mg	V/O	Mg/O
3V–Mg–O	0.09	0.10	1.12
8V–Mg–O	0.06	0.07	1.30
24V–Mg–O	0.20	0.16	0.81
35V–Mg–O	0.42	0.25	0.60
54V–Mg–O	0.40	0.29	0.72

[a] Calculated from Auger peak-to-peak intensities and the atomic sensitivity factors.

microscopic investigation are shown in Fig. 2. They show that the morphology of the catalyst particles depended on the vanadium content. Pure MgO particles were porous, fluffy, and round-shaped, about 20 μm in size (Fig. 2A). Addition of a small amount of vanadium resulted in samples containing particles of less uniform size and shape, as seen in Figs. 2B–E. Figures 2B and C show clearly that the 8V–Mg–O and 24V–Mg–O samples contained both rod-shaped and porous irregular particles. An examination of a particle in the 24V–Mg–O sample showed that the particle was not a well-formed crystal, but porous (Fig. 2D). The picture of the 54V–Mg–O sample shows that the sample consisted of mainly rod-shaped particles. Again, close examination of one particle showed that it was spongy and porous.

Reaction Study

The catalysts containing vanadium are generally very active beginning at about 500°C. Oxidative dehydrogenation and combustion are the major reactions. Table 4 shows the reaction products from the various cataylsts at 540°C. They are also plotted as a function of catalyst composition in Fig. 3. On the V–Mg–O catalysts, 1-butene, *cis*- and *trans*-2-butene, butadiene, CO, and CO_2 are always the major products. Small amounts of ethane and ethene (which were not separated) and propane and propene were also observed. Since the carbon balance based on the products listed was satisfied in all runs to within ±5%, no attempt was made to collect any condensable products.

As shown in Table 4 and Fig. 3, unsupported vanadium oxide showed low activity and low selectivity for oxidative dehydrogenation. The selectivity was low even at low conversions, and the dehydrogenation product was 1-butene. Interestingly, a much higher selectivity to C_3 products was observed at low conversion than at high conversion. A small amount of butadiene was also produced at high conversion. For MgO, the activity and the dehydrogenation selectivity were also low, and the dehydrogenation products were also butenes. A substantial selectivity for the cracked products was also observed.

TABLE 4

Conversion and Selectivity in Butane Oxidative Dehydrogenation over V–Mg–O[a]

Catalyst	Weight[b] (g)	Conversion (%)		Selectivity (%) (C_4 basis)								
		O_2	C_4H_{10}	CO	CO_2	C_2	C_3	1-C_4H_8	*trans*-2-C_4H_8	*cis*-2-C_4H_8	C_4H_6	Dehyd.[c]
MgO	1.9[d]	17	10.5	21.1	34.5	11.2	19.8	5.0	5.0	0	0	10.0
V_2O_5	0.2[d]	6	3.7	0	35	0	35	17	0	0	0	17
	0.4[d]	15	5.1	0	54	0	25	18	0	0	0	18
	1.9[d]	—	48.2	23.4	65.1	0	0.6	3.5	3.3	2.7	1.4	10.9
MgO + V_2O_5	0.5+ 0.95[d]	99	41	15.9	69.8	1.2	1.2	3.4	4.0	2.2	2.2	11.8
3V–Mg–O	0.3	85	35.5	24.9	50.7	6.8	4.3	5.5	1.5	1.3	4.3	12.6
8V–Mg–O	0.3	97	50.9	19.7	42.7	3.2	1.8	4.6	3.3	3.2	20.4	31.5
19V–Mg–O	0.3	97	58.7	15.3	31.8	2.3	1.0	7.0	1.8	2.3	37.7	48.8
	0.1	46	34.2	12.4	24.3	2.4	4.9	14.4	4.9	5.5	30.8	55.6
24V–Mg–O	0.1	95	56.2	17.0	30.1	1.8	0.8	7.9	2.3	2.7	37.2	50.1
35V–Mg–O	0.1	66	42.1	17.0	26.6	2.4	1.7	12.0	3.9	4.7	31.2	51.8
54V–Mg–O	0.1	42	31.3	15.9	21.9	2.8	5.1	15.9	6.2	7.2	24.2	53.5

[a] Reaction temperature: 540°C; feed: 4% butane and 8% O_2 in He.

[b] Unless noted, the catalysts were diluted with twice the weight of silica.

[c] Total selectivity to form butenes and butadiene.

[d] Undiluted with silica.

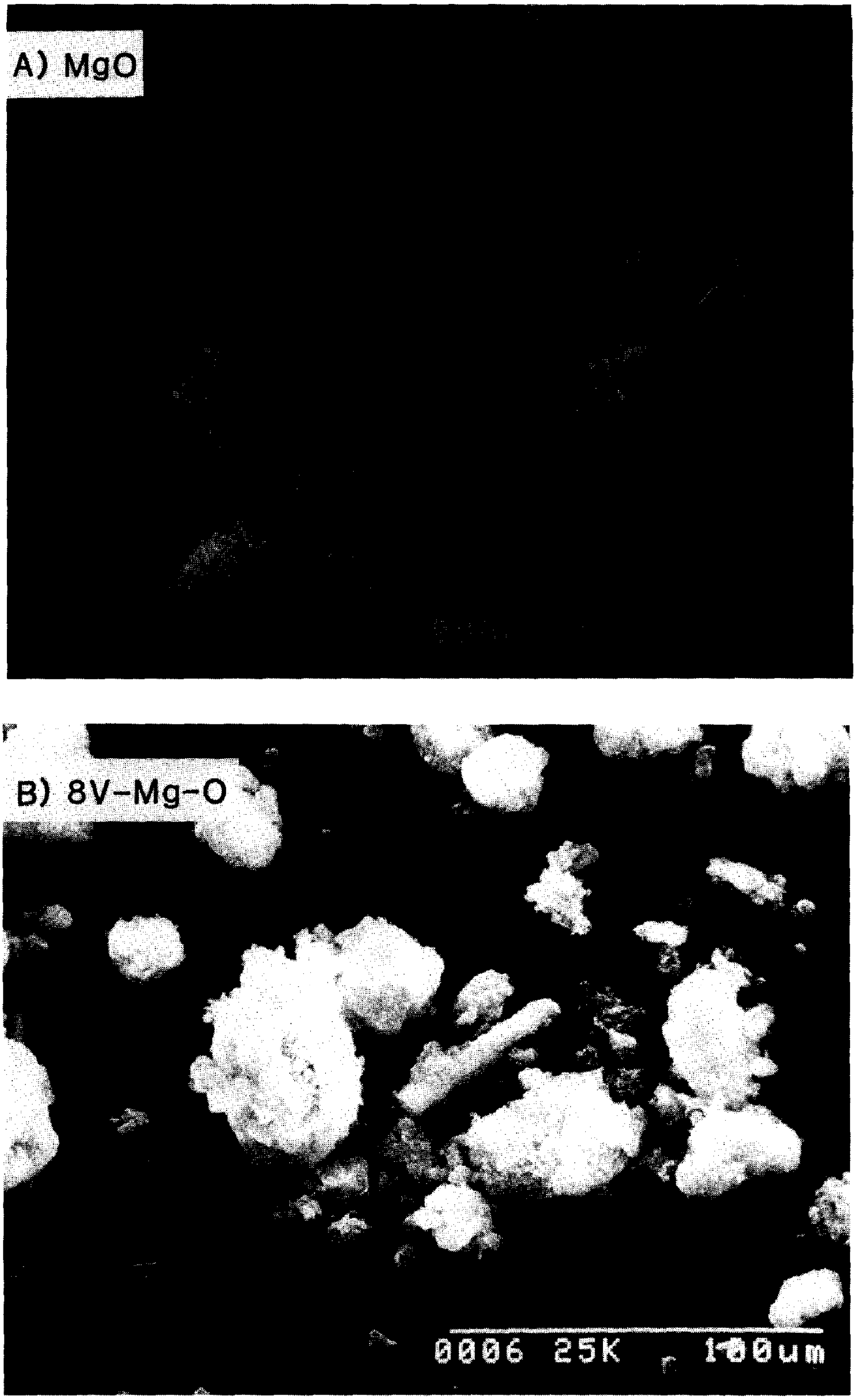

FIG. 2. Scanning electron micrographs of catalyst samples as prepared: (A) MgO, (B) 8V–Mg–O, (C, D) 24V–Mg–O, (E) 35V–Mg–O, (F, G) 54V–Mg–O.

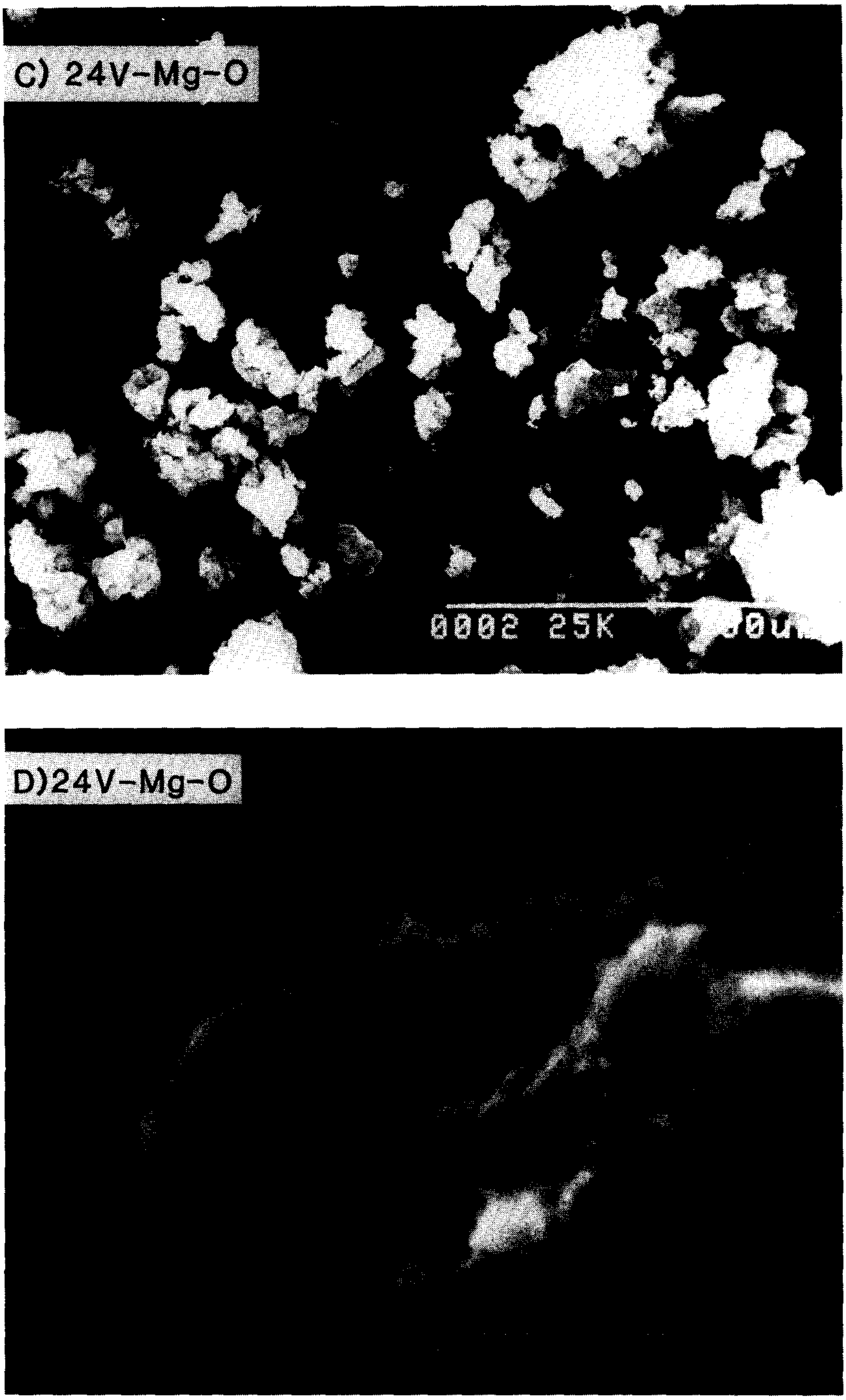

FIG. 2—*Continued.*

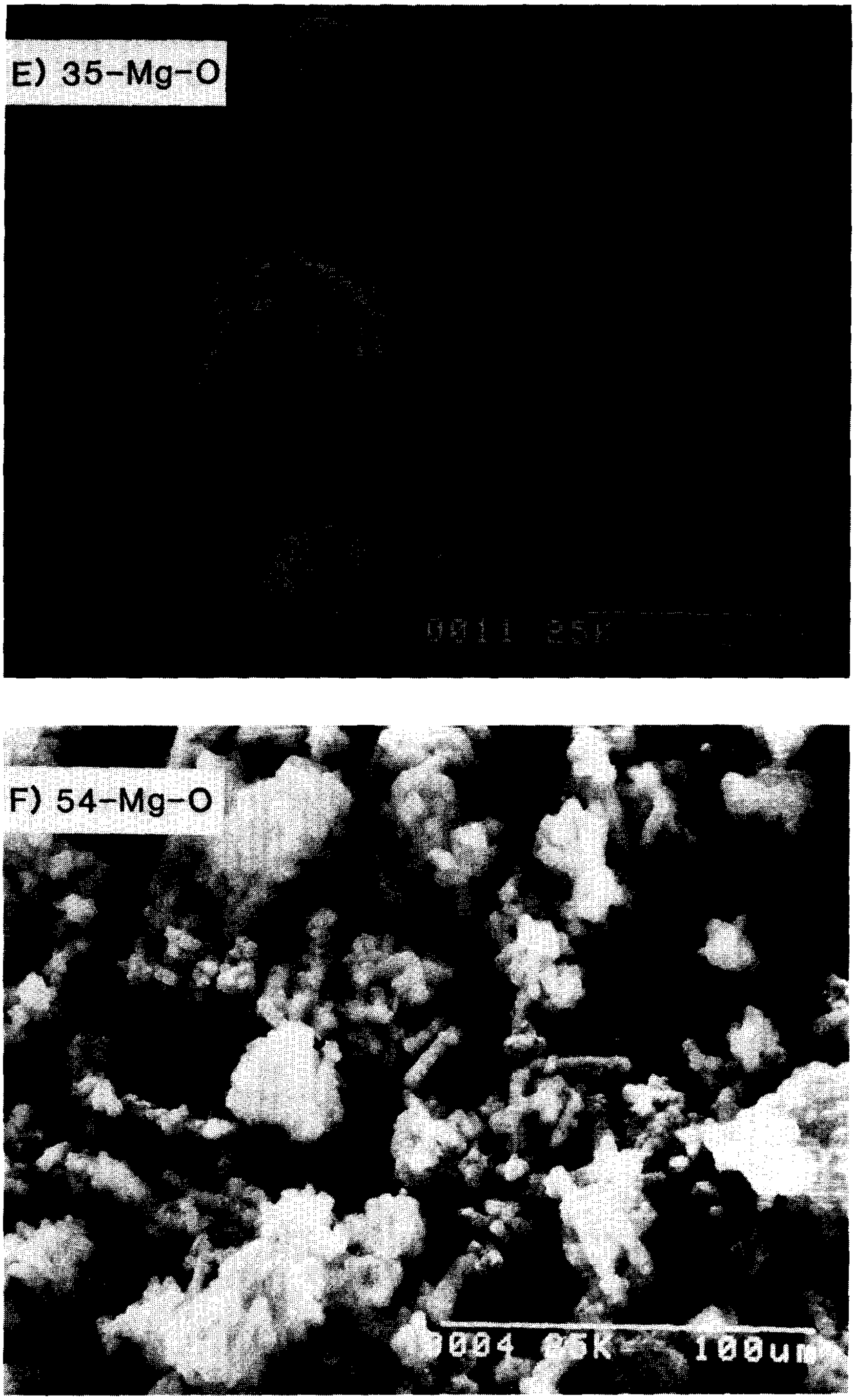

FIG. 2—*Continued.*

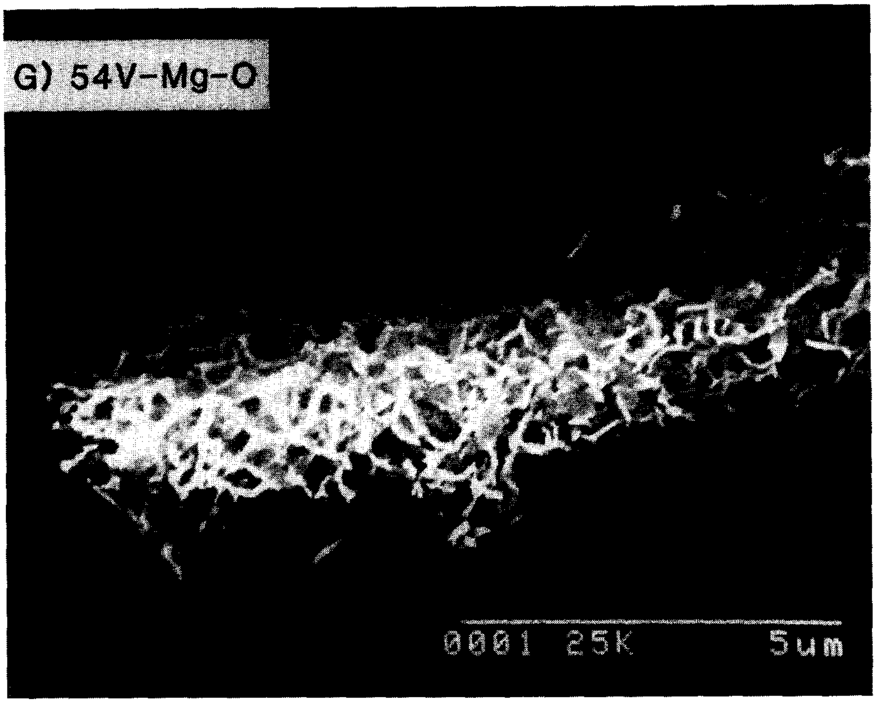

FIG. 2—*Continued.*

The behavior of a physical mixture of V_2O_5 and MgO was well described by the summation of the behavior of the pure components.

For the mixed oxide catalysts, the selectivity for oxidative dehydrogenation increased markedly with increasing vanadium content. At 3.5% vanadium, there was only a small increase in the selectivity compared with MgO. More significantly, there was a distinct increase in the selectivity for butadiene, and a substantial increase in the activity of the catalyst. As the vanadium content increased to 19%, the selectivity for butadiene increased to higher than 30%, while the total selectivity for dehydrogenation increased to about 50% at the expense of all other reaction products. The activity and the selectivity stayed at these high levels for catalysts of higher vanadium content.

Table 5 shows the data on the effect of conversion. If the oxygen conversion was substantially less than 100%, the selectivity for butadiene increased with increasing conversion, while the total selectivity for dehydrogenation decreased. If the amount

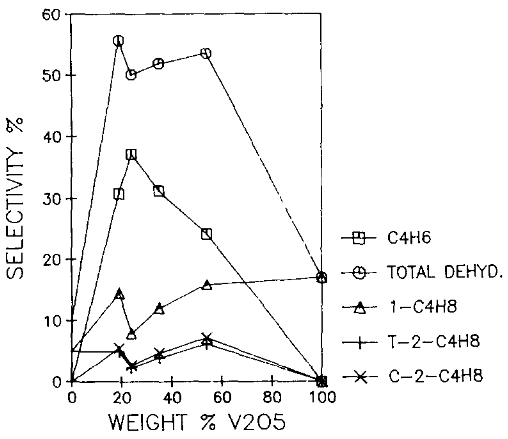

FIG. 3. Selectivity for butadiene, butenes, total dehydrogenation as a function of catalyst composition. Data are for 540°C; 4% butane, 8% O_2, in He; 0.1 g catalyst, except MgO, which is for 1.9 g, and V_2O_5, which is for 0.2 g.

TABLE 5

Effect of Conversion on the Selectivity (Catalyst: 19V–Mg–O)[a]

Weight[b] (g)	Conversion (%)		Selectivity (%) (C_4 basis)								
	O_2	C_4H_{10}	CO	CO_2	C_2	C_3	1-C_4H_8	*trans*-2-C_4H_8	*cis*-2-C_4H_8	C_4H_6	Dehyd.[c]
0.5[d]	98	59.2	16.5	36.8	2.8	0.7	5.8	1.8	2.1	33.2	42.9
0.5	98	57.3	15.7	34.2	2.6	1.1	6.6	2.1	2.6	34.9	46.2
0.3	97	58.7	15.3	31.8	2.3	1.0	7.0	1.8	2.3	37.7	48.8
0.2	73	47.2	14.9	30.8	2.0	2.0	9.7	2.8	3.6	33.5	49.6
0.1	46	34.2	12.4	24.3	2.4	4.9	14.4	4.9	5.5	30.8	55.6

[a] Reaction temperature: 540°C; feed: 4% butane, 8% O_2, 88% He.

[b] Unless specified, the catalysts were diluted with twice the weight of SiO_2.

[c] Total selectivity to butenes and butadiene.

[d] Undiluted samples.

of catalyst was more than enough for complete oxygen conversion, the selectivity for butenes and butadiene decreased slightly. Presumably, in the region of the catalyst bed where there was no gaseous oxygen, the reaction products could reduce the catalyst and form carbon oxides. Indeed, in such a circumstance, the portion of the catalyst nearer the reactor outlet turned bluish gray after reaction. This indicated the reduction of V(V) to lower oxidation states.

The effect of temperature was also investigated and the results are shown in Table 6. As expected, an increase in the temperature resulted in an increase in the conversion. This was achieved with only a small penalty in the selectivity for dehydrogenation. The selectivity for butadiene actually increased, while those of the butenes decreased. There was a slight increase in the selectivity for the combustion products, and the selectivity for the cracked products remained small.

Finally, Table 7 shows the effect of the oxygen-to-butane ratio in the feed. This

TABLE 6

Effect of Temperature in Butane Oxidation over V–Mg–O[a]

Catalyst[b]	T (°C)	Conversion (%)		Selectivity (%) (C_4 basis)								
		O_2	C_4H_{10}	CO	CO_2	C_2	C_3	1-C_4H_8	*trans*-2-C_4H_8	*cis*-2-C_4H_8	C_4H_6	Dehyd.[c]
19V–Mg–O	510	23	18.7	14.3	19.8	1.2	5.5	18.0	7.4	8.1	21.7	55.2
	540	46	34.2	12.3	24.3	2.4	4.9	14.4	4.9	5.5	30.8	55.6
	570	83	53.7	15.3	26.6	3.1	3.7	8.9	2.6	3	36.1	50.6
	600	98	63.3	15.8	27.0	4.1	1.5	7.6	2.1	2.6	38.7	51.0
24V–Mg–O	480	27	10.9	4.9	30.8	0	4.9	11.0	8.5	8.5	25.8	53.8
	510	64	40.5	15.8	29.7	1.2	0.8	11.4	3.6	4.5	32.9	52.4
	540	95	56.2	17.0	30.1	1.8	0.8	7.9	2.3	2.7	37.2	50.1
35V–Mg–O	510	31	23.0	14.1	22.7	2.0	4.5	17.1	7.1	8.0	23.1	55.3
	540	66	42.1	17.0	26.6	2.4	1.7	12.0	3.9	4.7	31.2	51.8
	570	99	61.7	18.5	27.3	3.2	1.3	7.1	2.1	2.5	37.6	49.3
54V–Mg–O	510	21	17.6	14.4	21.4	2.8	7.0	18.7	8.4	9.3	16.8	53.2
	540	42	31.3	15.9	21.9	2.8	5.1	15.9	6.2	7.2	24.2	53.5

[a] Feed: 4% butane, 8% O_2, 88% He.

[b] 0.1 g catalyst diluted with 0.2 g silica.

[c] Total selectivity for butenes and butadiene.

TABLE 7

Effect of Feed Composition in Butane Oxidation on V–Mg–O (Catalyst: 19V–Mg–O)[a]

Feed C_4H_{10}/O_2	Conversion (%)		Selectivity (%) (C_4 basis)								
	O_2	C_4H_{10}	CO	CO_2	C_2	C_3	1-C_4H_8	*trans*-2-C_4H_8	*cis*-2-C_4H_8	C_4H_6	Dehyd.
4/8	73	47.2	14.9	30.8	2	2	9.7	2.8	3.6	33.5	49.6
4/6	83	42.7	13.2	27.5	1.9	3.0	11.4	3.3	4.2	35.2	54.1
4/4	95	28.5	10.2	11.5	1.5	4.5	16.2	5.6	6.9	31.7	60.4

[a] Reaction temperature: 540°C, feed: 4% butane, varying O_2, balance He. 0.2 g catalyst diluted with 0.4 g silica.

ratio was varied by changing the partial pressure of oxygen while keeping the partial pressure of butane fixed. With a decreasing oxygen-to-butane ratio, the butane conversion decreased whereas the oxygen conversion increased. The total selectivity for dehydrogenation also increased mostly due to the increase in butenes. There might be a slight but not significant increase in the cracked products.

DISCUSSION

Nature of the Catalysts

The data presented in the reaction studies clearly show that the V–Mg–O catalysts are quite selective for the oxidative dehydrogenation of butane to butenes and butadiene. Interestingly, however, within experimental error, there are no oxygenation products. In this sense, the catalysts are very different from the unsupported V_2O_5, V_2O_5/TiO_2, or V_2O_5/Al_2O_3 catalysts which catalyze the oxidation of butenes and butadiene to maleic anhydride at temperatures below 500°C (*8*). Unsupported V_2O_5 is nonselective in the oxidation of butane (*8*, *9*). The V–Mg–O catalysts are also different from V–P–O which catalyzes the oxidation of butane to maleic anhydride (*14*). Such a different catalytic behavior suggests a strong interaction between vanadium oxide and magnesium oxide that is not found in the other catalysts.

It is well established that V_2O_5 forms a layer structure on anatase titania and alumina to expose the (010) plane preferentially (*15*, *16*). There is a high density of V=O groups on this (010) plane. The V=O groups possess a characteristic infrared stretching frequency at 1022 cm^{-1}. As shown in Fig. 1, this characteristic V=O stretching is not observed in the V–Mg–O samples. Thus the vanadium oxide in V–Mg–O does not form a layer structure on the MgO substrate. This picture is further supported by the fact that the catalyst particles of V–Mg–O are very different from the fluffy round particles of MgO, and the fact that Auger spectroscopy shows the presence of substantial amounts of Mg on the particle surface even with very high vanadium loadings. This conclusion has also been arrived at by Iwamoto *et al.* (*17*) and Hanuza *et al.* (*11*). The latter authors have further proposed that the catalyst is magnesium orthovanadate, $Mg_3(VO_4)_2$.

Our data support the proposal that magnesium orthovanadate is the active component. The presence of this compound was detected by X-ray diffraction (Table 2). No compounds other than MgO were detected. That magnesium orthovanadate is formed instead of $Mg_2V_2O_7$ and MgV_2O_6 is reasonable. In our samples, the highest concentration of vanadium is 20.4 mol% V_2O_5 in the 54V–Mg–O sample. At this composition, MgO and $Mg_3(VO_4)_2$ are the stable phases (*18*).

Infrared spectroscopy also supports the formation of this compound. Baran *et al.* (*19*) and Hanuza *et al.* (*11*) reported the spectrum of magnesium orthovanadate, which is characterized by two strong and broad absorption bands. The first band due to the ν_3 antisymmetric stretch of $(VO_4)^{3-}$ anions (*20*) centers at 860 cm^{-1} (*19*) or 863 cm^{-1} (*11*). The second band centers at 695 cm^{-1} and is assigned to the V–O–V stretch by Hanuza *et al.* and to the tetrahedral MgO_4 stretch by Baran *et al.* Both strong bands are observed in our V–Mg–O samples of more than 24 wt% V_2O_5. Hanuza *et al.* also reported the spectra for $Mg_2V_2O_7$ and MgV_2O_6 (*11*). These spectra show absorption bands in the region 500–600 cm^{-1} that are absent in the orthovanadate spectrum. The absence of absorption in this region in our samples of high vanadium content thus excludes the presence of metavanadate and pyrovanadate, consistent with the X-ray diffraction data.

In our samples of high vanadium content, the peak around 690 cm^{-1} is composed of two peaks located at 690 and 718 cm^{-1}. The two peaks may reflect the presence of different degrees of distortion of the orthovanadate structure. The ν_3 antisymmetric stretch of $(VO_4)^{3-}$ appears as the most dominant peak at 855 to 861 cm^{-1}. The ν_1 symmetric stretch appears as the shoulder at 920 cm^{-1}.

The spectrum for the 8V–Mg–O sample does not resemble those of any known magnesium vanadates. Its 731 cm^{-1} band is more intense than the 895 cm^{-1} band. The spectrum for the 19V–Mg–O sample is complex, but except for the 820 cm^{-1} peak, it may be explained by a combination of the spectra for 8V–Mg–O and 24V–Mg–O. In view of the lack of evidence for the presence of any compounds other than magnesium orthovanadate, we suggest tentatively that these spectra are due to highly dispersed and highly distorted magnesium orthovanadate on a MgO support.

The scanning electron micrographs (Fig. 2) support the conjecture of the presence of distorted magnesium orthovanadate. The micrographs show that the particles are porous instead of crystalline. This is consistent with the high surface areas of the samples (Table 1). These micrographs further show the formation of rod-shaped particles in samples containing vanadium. The 54V–Mg–O sample consists of almost entirely these rod-shaped particles, which in view of the X-ray and IR results can be assigned to magnesium orthovanadate.

Results of Auger spectroscopy also support the formation of a vanadium–magnesium compound. The surface V/Mg ratio approaches a constant value at a high vanadium loading. This is expected if a compound is formed. It also excludes the formation of a layer structure of V_2O_5 on MgO, which would show a much higher V/Mg ratio than observed.

In this manner, the V–Mg–O system differs from the other supported vanadium oxides. The role of MgO is not to induce the preferential formation of a particular surface-exposed plane of V_2O_5, or to modify the reactivity of the V=O group on this exposed plane. The system also differs from the Ni–Mo–O system where the role of NiO is to form a much less active $NiMoO_4$ that preferentially blocks the combustion sites on MoO_3 (*21*). Instead, the active and selective phase is the compound magnesium orthovanate.

Reaction Mechanism

It has been shown by deuterium isotope effects at different positions of the carbon chain that the first step in the selective oxidation of butane to maleic anhydride on a V–P–O catalyst is similar to a free radical reaction (*22*). That this should be a free radical type of reaction instead of an acid–base type has also been suggested based on energetic arguments (*23*). It is reasonable to assume the same activation step for butane in this study. Thus butane is activated by the catalyst that abstracts a H atom from the molecule to form an adsorbed butyl radical and a surface OH group. Such a step requires the presence on the surface of a very reactive oxygen, such as an O^- species. This species can be supplied by the decomposition of N_2O when it is used as the oxidant (*1–3*). In this study, it can be formed by the charge transfer reaction

$$V^{5+}O^{2-} \rightarrow V^{4+}O^{-}.$$

The presence of this species at surface defect sites is also possible.

It is interesting that 1-butene is formed preferentially to *cis*- and *trans*-2-butene. In fact, the ratio of 1-butene : *cis*-2-butene : *trans*-2-butene is almost always 3 : 1 : 1. That can be explained by the following. Butane first reacts by the dissociation of a methylene C–H bond to form a secondary butyl radical. That this is the predominant pathway has been confirmed by the deuterium isotope effect on V–P–O catalyst (*22*). The butyl radical formed is very reactive. It forms butenes by losing another hydrogen from the carbon atoms adjacent to the first carbon site:

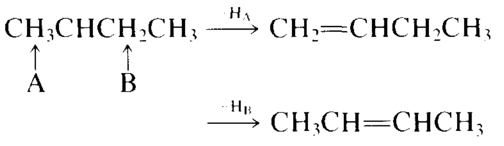

$$\underset{\substack{\uparrow\\ A}}{CH_3}\dot{C}H\underset{\substack{\uparrow\\ B}}{CH_2}CH_3 \xrightarrow{-H_A} CH_2{=}CHCH_2CH_3$$
$$\xrightarrow{-H_B} CH_3CH{=}CHCH_3$$

Loss of any one of the three hydrogens at position A leads to 1-butene. Loss of one of the hydrogens at position B leads to *cis*-2-butene, and loss of the other hydrogen at position B leads to *trans*-2-butene. If this hydrogen loss step is very rapid, and the hydrogen is lost statistically, the butene isomers will be in the observed ratio of 3 : 1 : 1, which is different from the equilibrium ratio of 1 : 1.0 : 1.1.

Further dehydrogenation of butene to butadiene could take place with and without the desorption of butenes. Indeed, butene can be oxidatively dehydrogenated to butadiene on V–Mg–O with reasonable selectivity (about 50%) (*12*), which has been confirmed in our laboratory. The relatively small dependence of butadiene and butene selectivity on conversion and temperature (Tables 4 to 7) suggests that the formation of butadiene as a secondary product of butenes that desorbed and then readsorbed is not the only dominant route for butadiene formation. That is, the formation of butadiene as the initial reaction product is also significant.

Selectivity for Oxidative Dehydrogenation

It is very interesting that for the V–Mg–O catalysts, oxidative dehydrogenation is the primary selective oxidation reaction. While on other vanadium oxide-containing catalysts maleic anhydride is formed from butane, butenes, and butadiene, little or no oxygenate is formed over V–Mg–O. It is worthwhile to speculate why oxygenates are not formed on this catalyst.

The difference between the V–Mg–O catalyst and the others must lie in the different reactivity toward butenes and butadiene, which is low on V–Mg–O and high on the other vanadium catalysts. We propose two possible contributing factors. The first factor is the fact that butenes and butadiene adsorb much more weakly on V–Mg–O. The second factor is that the V–Mg–O surface contains less and/or less active oxygen for oxidation.

Due to the high electron densities at the π bonds in butenes and butadiene, these molecules are considered basic or nucleophilic. Vanadium oxide is acidic. Magnesium oxide, on the other hand, is basic. By forming magnesium orthovanadate, much of the acid property of the vanadium oxide is removed. In fact, the catalyst is probably basic. Thus butenes and butadiene adsorb weakly on this basic oxide, which results in their much lower reactivity. They become significant products.

Vanadium oxide and V–P–O are not basic. It is likely that butene and butadiene interact much more strongly with them than with V–Mg–O. The result is a much longer surface residence time for these molecules, which significantly increases their probability of being further oxidized.

As to the second factor concerning the surface active oxygen, it has been shown that the activity of V_2O_5, either unsupported or supported on TiO_2 or Al_2O_3, can be correlated with the amount of V=O in the sample (*16, 17, 24*). This V=O is characterized by an IR band at around 1022 cm^{-1}. It is also present on V–P–O (*25*). From the crystal structure, the surface density of adjacent V=O is higher on V_2O_5 than on V–P–O (*26, 27*). However, there is no V=O on magnesium orthovanadate where the shortest V–O bond has a bond order of 1 · 5, and its density is substantially lower than that of the V=O in V_2O_5 (*28*). If this V=O is important for oxygenate formation, the different V–O bond character and its lower density on V–Mg–O may account for the absence of oxygenate formation.

In summary, the high selectivity for oxidative dehydrogenation of butane on V–Mg–O is due to the intimate presence of both vanadium oxide and magnesium oxide found in the compound magnesium orthovanadate. The vanadium–oxygen centers are necessary to activate butane, while the MgO component is necessary to modify the acidic property of vanadium oxide and to reduce the reactivity and density of surface V=O species. The result is a much lower reactivity of butenes and butadiene on this catalyst than V_2O_5 or V–P–O. This model would suggest that the V–Mg–O catalysts are also selective oxidative dehydrogenation catalysts for other alkanes. Indeed, rather good selectivities have been observed for propane and isobutane. These results will be separately reported.

ACKNOWLEDGMENTS

Support of this work by the Department of Energy, Basic Energy Sciences Division, is gratefully acknowledged. The authors also thank Kam Lui and Mai Nguyen for their experimental assistance.

REFERENCES

1. Mendelovici, L., and Lunsford, J. H., *J. Catal.* **94,** 37 (1985); Ward, M. B., Lin, M. J., and Lunsford, J. H., *J. Catal.* **50,** 306 (1977).
2. Liu, R. S., Iwamoto, M., and Lunsford, J. H., *J. Chem. Soc. Chem. Commun.,* 78 (1982).
3. Lin, H. F., Liu, R. S., Liew, K. Y., Johnson, R. E., and Lunsford, J. H., *J. Amer. Chem. Soc.* **106,** 4117 (1984).
4. Khan, M. M., and Somorjai, G. A., *J. Catal.* **91,** 263 (1985).
5. Zhen, K. J., Khan, M. M., Mak, C. H., Lewis, K. B., and Somorjai, G. A., *J. Catal.* **94,** 501 (1985).
6. Stepanov, G. A., Tsailingol'd, A. L., Levin, V. A., and Pilipenko, F. S., *Stud. Surf. Sci. Catal.* **7** (Pt. B, *New Horizon Catal.*), 1293 (1981).
7. Doroshenko, V. A., Shapovalova, L. P., and Tmenov, D. N., *Z. Prik, Khim.* **55,** 80 (1982).
8. Mori, K., Miyamoto, A., and Murakami, Y., *Appl. Catal.* **6,** 209 (1983).
9. Bretton, R. H., Wan, S.-W., and Dodge, B. F., *Ind. Eng. Chem.* **44,** 594 (1952).
10. Oganowski, W., Nowicki, A., and Hanuza, J., *Bull. Pol. Acad. Sci. Chem.* **31,** 129 (1984).
11. Hanuza, J., Jezowska-Tryebratowska, B., and Oganowski, W., *J. Mol. Catal.* **29,** 109 (1985).
12. Simakov, A. V., and Veniaminov, S. A., *React. Kinet. Catal. Lett.* **28,** 67 (1985).
13. "Handbook of Auger Electron Spectroscopy," Physical Electronics Industry, Inc., 1978.
14. Hodnett, B. K., *Catal. Rev.* **27,** 373 (1985).
15. Miyamoto, A., Yamazaki, Y., Inomata, M., and Murakami, Y., *J. Phys. Chem.* **85,** 2366 (1981).
16. Inomata, M., Miyamoto, A., and Murakami, Y., *J. Phys. Chem.* **85,** 2372 (1981).
17. Iwamoto, M., Takenaka, T., Matsukami, K., Hirata, J., Kagawa, S., and Izumi, J., *Appl. Catal.* **16,** 153 (1985).
18. Kerby, R. C., and Wilson, J. R., *Canad. J. Chem.* **51,** 1032 (1973).
19. Baran, E. J., Tentil, L. A., Pedregosa, J. C., and Aymonino, P. J., *Z. Anorg. Allg. Chem.* **365,** 213 (1969).
20. Griffith, W. P., and Gonzales, F., *J. Chem. Soc. Dalton Trans.,* 1416 (1972).
21. Ozkan, U., and Schrader, G. L., *J. Catal.* **95,** 120, 137, 147 (1985).
22. Pepera, M. A., Callahan, J. L., Desmond, M. J., Milburger, E. C., Blum, P. R., and Bremer, N. J., *J. Amer. Chem. Soc.* **107,** 4883 (1985).
23. Kung, H. H., *Ind. Eng. Chem. Prod. Res. Dev.* **25,** 171 (1986).
24. Mori, K., Miyamoto, A., and Murakami, Y., *J. Chem. Soc. Faraday Trans. 1* **82,** 13 (1986).
25. Moser, T. P., and Schrader, G. L., *J. Catal.* **92,** 216 (1985).
26. Wells, A. F., "Structural Inorganic Chemistry," 4th ed. Oxford University Press (Clarendon), London/New York, 1975.
27. Busca, G., Centi, G., Trifiro, F., and Lorenzellli, V., *J. Phys. Chem.* **90,** 1337 (1986).
28. Krishnamachari, N., and Calvo, C., *Canad. J. Chem.* **49,** 1629 (1971).